2D laser lithography on silicon substrates via photoinduced copper-mediated radical polymerization

Peer-reviewed author version

LAUN, Joachim; De Smet, Yana; Van de Reydt, Emma; KRIVCOV, Alexander; Trouillet, Vanessa; Welle, Alexander; Möbius, Hildegard; Barner-Kowollik, Christopher & JUNKERS, Tanja (2018) 2D laser lithography on silicon substrates via photoinduced copper-mediated radical polymerization. In: CHEMICAL COMMUNICATIONS, 54 (7), p. 751-754.

DOI: 10.1039/c7cc08444g
Handle: http://hdl.handle.net/1942/25575

Chemical Communications

COMMUNICATION

2D Laser Lithography on Silicon Substrates via Photoinduced Copper-Mediated Radical Polymerization†

Received 00th January 20xx,
Accepted 00th January 20xx

DOI: 10.1039/x0xx00000x

www.rsc.org/

Joachim Laun,[a] Yana De Smet,[a] Emma Van de Reydt,[a] Alexander Krivcov,[b] Vanessa Trouillet,[c,d] Alexander Welle,[d,e] Hildegard Möbius,[b] Christopher Barner-Kowollik[f,g,h]* and Tanja Junkers[a,i]*

A 2D laser lithography protocol for controlled grafting of polymer brushes in a single-step is presented. A series of polyacrylates were grafted from silicon substrates via laser-induced copper-mediated radical polymerization. Film thicknesses up to 39 nm were reached within 125 µs of exposure to UV laser light (351 nm). Successful block copolymerization underpinned the controlled nature of the grafting methodology. The resolution of a small structure of grafted PHEA reached 270 µm and was limited by the type of laser used in the study. Further, a checkerboard pattern of PtBA and POEGA was produced and imaged via time-of-flight secondary ion mass spectrometry (ToF-SIMS), and X-ray photoelectron spectroscopy (XPS).

The need for polymer-patterned surfaces has been growing over the past twenty years as interactions between two materials are largely determined by their surface characteristics.[1] Grafting of polymer brushes onto surfaces hereby often provides good control over optical and mechanical surface properties and is hence ideal to tailor surface properties in a wide range of applications.

Polymer brushes are typically obtained via two pathways: Grafting-from or grafting-to approaches.[2] Grafting-to reactions proceed via efficient conjugations, attaching a preformed polymer to the surface. While overall quite versatile, grafting-to often leads to comparatively low grafting densities due to steric congestion.[3-5] On the other side, the employed polymers can be synthesized in solution and therefore excellent control of the grafted material is obtained. Grafting-from reactions build polymeric structures from the surface and provide good control over film thickness, composition and architecture while concomitantly yielding high grafting densities.[6] However, grafting-from usually leads to less defined polymer microstructures because surface-initiated polymerization kinetics can differ significantly from solution-based reactions.[7] Further, surface characterization is inherently more challenging, which often leaves uncertainty about the exact composition and structure of grafted-from brushes.

With the discovery of living and controlled polymerization protocols, well-defined and tailor-made polymeric architectures have become accessible.[8] Especially reversible-deactivation radical polymerization (RDRP) with its high tolerance towards chemical functionalities and the availability of straightforward reaction protocols has become the tool of choice for surface engineering.[6, 9] The three most widely used RDRPs are reversible-addition fragmentation transfer radical polymerization (RAFT),[10] nitroxide-mediated polymerization (NMP),[11] and atom transfer radical polymerization (ATRP) which is often – but not exclusively – conducted with copper catalyst.[12] Precise control over chain length, dispersity, and chemical functionalities is an essential but not sufficient feature to obtain well-defined polymer patterns. Spatial control on flat substrates is equally important and can be realized via various techniques,[13] such as microcontact printing,[14] dip pen[15] or polymer pen lithography,[16, 17] conventional lithography with a photomask and resist,[18] or light-induced reaction[19] to only mention a few. Light-induced reactions are especially interesting thanks to simple procedures, good scalability, and additional temporal control.

[a] Polymer Reaction Design Group, Institute for Materials Research (IMO), Universiteit Hasselt, Martelarenlaan 42, 3500 Hasselt, Belgium
E-mail: tanja.junkers@uhasselt.be
[b] University of Applied Sciences Kaiserslautern, 66482 Zweibrücken, Germany
[c] Institute for Applied Materials (IAM), Karlsruhe Institute of Technology (KIT), Hermann-von-Helmholtz-Platz 1, 76344 Eggenstein-Leopoldshafen, Germany
[d] Karlsruhe Nano Micro Facility (KNMF), Karlsruhe Institute of Technology (KIT), Hermann-von-Helmholtz-Platz 1, 76344 Eggenstein-Leopoldshafen, Germany
[e] Institute of Functional Interfaces, Karlsruhe Institute of Technology (KIT), Hermann-von-Helmholtz-Platz 1, 76344 Eggenstein-Leopoldshafen, Germany
[f] School of Chemistry, Physics and Mechanical Engineering, Queensland University of Technology (QUT), 2 George Street, QLD 4000 Brisbane, Australia
E-mail: christopher.barnerkowollik@qut.edu.au
[g] Macromolecular Architectures, Institut für Technische Chemie und Polymerchemie, Karlsruhe Institute of Technology (KIT), Engesserstraße 18, 76128 Karlsruhe, Germany, christopher.barner-kowollik@kit.edu
[h] Institut für Biologische Grenzflächen (IBG), Karlsruhe Institute of Technology (KIT), Hermann-von-Helmholtz-Platz 1, 76344 Eggenstein-Leopoldshafen, Germany
[i] IMEC associated lab IMOMEC, Wetenschapspark 1, 3590 Diepenbeek, Belgium
† Electronic Supplementary Information (ESI) available: See DOI: 10.1039/x0xx00000x

Combining tunable material properties with spatial control via the use of light, photoRDRP has become a powerful tool for surface engineering.[19] PhotoRDRP was successfully employed to graft polymer brushes of different length and block copolymers of methacrylates, using iridium catalysts[20, 21] and metal-free systems.[22, 23] Photo-induced copper-mediated radical polymerization (photoCMP) has been reported for polyacrylates[24] and polymethacrylates.[25, 26] Films up to almost 1 µm thickness of polyacrylates were produced at lowest catalyst concentrations.[24] Up to now, spatial control was achieved via the use of conventional photomasks. Even though some very convincing examples of spatial control have been reported recently for iridium catalysts combined with inkjet-printed photomasks in a stop-flow cell,[21] photomask-free procedures such as laser lithography are more versatile and allow for fast adaptions.

To date, there are only few examples that combine 2D laser lithography on flat surfaces and RDRP. Very recently, polymer brushes with close to 50 nm resolution were grafted in a two-step procedure by the Barner-Kowollik and Wegener teams: stimulated-emission depletion was exploited in two photon laser lithography to graft an ATRP initiator, which was followed by thermal surface-initiated CMP.[27] Using photoRDRP, also one-step methodologies towards well-resolved polymer structures were reported, yet actual photoRDRP characteristics (controlled chain growth and end group fidelity) have never been confirmed. PhotoNMP of di- and triacrylates was employed to graft a multilayered, µm-resolved network structure from a crosslinked polymer film.[28] Control over film thickness was hereby obtained by adjustment of the exposure time on a millisecond scale and the technique was not tested for brush-like (hence non-crosslinking monomers) structures. More recently, the same group reported an iridium-based system to graft micrometer-resolved structures via laser lithography from crosslinked polymer films.[29] Good control over film thickness was achieved by variation of laser power for a constant exposure time of 5 ms, however, no information on the used monomer and no proof of RDRP-like behavior was provided.

Herein, we pioneer the combination of photoCMP with laser lithography, specifically for grafting-from of polymer brushes. RDRP-like behavior was convincingly demonstrated: Following a general grafting of polymer brushes for various acrylates, the kinetics for the grafting of PtBA brushes are investigated. Successful block copolymerization is evidenced via XPS and grazing angle attenuated total reflection Fourier-transform (GAATR-FTIR). Finally, the generation of different surface patterns is described and the resolution is assessed via ToF-SIMS.

The formation of polymer brushes on surfaces comprises a two-step procedure: first, the formation of a self-assembled monolayer of a covalently bonded suitable initiator and, second, the grafting-from polymerization. Stable self-assembled monolayers leading to high grafting densities of polymer brushes are generally obtained for

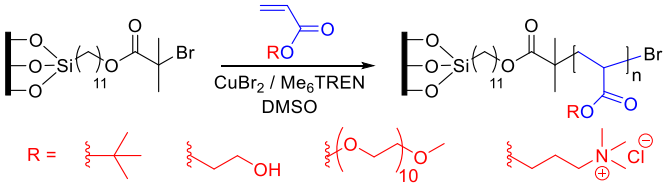

Scheme 1. Photoinduced copper-mediated radical polymerization for surface grafting of polyacrylates.

initiators with undecyl spacers between anchor group and initiating site.[6] We have chosen to work with 11-(trichlorosilyl)undecyl 2-bromo2-methylpropanoate to avoid poorly defined monolayers that are often obtained for triethoxysilanes.[30] PhotoCMP laser lithography was carried out with a pulsed excimer laser of 351 nm wavelength and a galvo scanner with focus lens to graft patterns of polymer onto modified flat silicon substrates.

We found the reaction to be oxygen sensitive, but insensitive towards water. **Scheme 1** depicts the performed grafting reaction. A range of acrylate monomers ranging from hydrophobic *t*-butyl acrylate (tBA) over more hydrophilic 2-hydroxyethyl acrylate (HEA) and oligo(ethylene glycol) methyl ether acrylate (OEGA) to very hydrophilic [2-(acryloyloxy)ethyl] trimethylammonium chloride (AETMAC) was polymerized in the presence of copper(II) bromide and tris[2-(dimethylamino)ethyl] amine (Me_6TREN) in DMSO upon exposure to laser light. For simplistic reasons and to account for non-ideal focus adjustment, we assume a focused beam size of 250 × 250 µm². The writing speed was set to 0.02 m·s^{-1} to achieve a homogenous light exposure despite the pulsed nature of the laser.

At first, the general feasibility of laser-induced copper-mediated radical polymerization was assessed. The above listed acrylates were grafted homogenously on a silicon substrate and confirmed by XPS. The left side of **Fig. 1** depicts the C 1s XPS spectrum of PtBA whose peak ratios are in excellent agreement with the theoretical values. XPS data for the remaining polymer grafts, additional ToF-SIMS, and GAATR-FTIR measurements are described in the Supporting Information (Fig. S3, Fig. S5, Fig. S7, and Table S1). Subsequently, the grafting kinetics of PtBA were investigated. On its right, **Fig. 1** shows the film thickness evolution of PtBA as a function of exposure time to direct light. Film thicknesses range from 0 nm after 8 µs up to 39 nm after 125 µs of laser light. Film thicknesses up to 190 nm could be obtained for longer reaction times (Fig. S2).

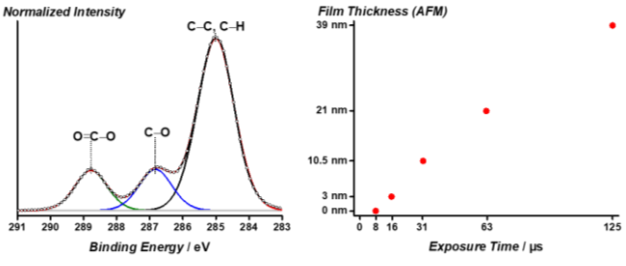

Fig. 1. (left) C 1s XPS spectrum of PtBA. (right) Evolution of PtBA film thickness with direct exposure time to laser light. Film thicknesses were determined via AFM scratch tests.

The film thickness evolution follows a linear slope, which is usually considered as indication for the livingness of the grafting process, since there is no noticeable decrease in monomer concentration and molecular weights can hardly be determined on flat surfaces. We note that kinetics in SI-CMP can different significantly from solution experiments.[31] The induction period of 8 µs was potentially caused by oxygen, similar observations are reported in literature.[29] Consequently, no film was grafted in the areas not exposed to laser light according to AFM. Interestingly, AFM did not show sharp edges but smooth transitions. While linear evolution of film thickness is a good indicator of controlled chain growth, block copolymer formation is typically regarded as further proof since it is used to assess reinitiation capabilities (and hence retention of the active chain end). Here, a rectangle of PtBA was grafted onto a silicon substrate and subsequently a smaller rectangle of PHEA was grafted in the middle of the larger one. A clearly visible change of hydrophilicity was observed during the subsequent washing procedure according to the grafted structure. GAATR-FTIR, ToF-SIMS and XPS confirm the successful formation of the block copolymer (Fig. S4, Fig. S6, and Table S1). The XPS spectrum of the diblock copolymer shows a mixture of both polymers since PtBA and PHEA are not phase separating. A carbon ratio C–O / O–C=O of 1.24 was found which corresponds to ≈56% PtBA and ≈44% PHEA within the uppermost 8 – 10 nm. In literature, 120 nm-thick PHEA-*b*-PtBA (with only 47 nm PtBA as first block) showed only 60% PHEA contribution to the XPS C 1s spectrum.[24] Therefore, we conclude that diblock copolymerization was successful also for laser lithography.

Finally, the resolution of the grafted polymer was assessed with a test structure typically used in photolithography (**Fig. 2**, top left): Starting from a small rectangle of 236 × 236 µm² in the upper left corner, a series of rectangles with increasing sizes and inter-rectangle distances along the respective x- and y-axis was created. Thus, we are able to monitor not only the lateral resolution, yet also the influence of the structure size. Each structure was exposed to laser light for 9 µs per surface area and HEA was used as monomer. The upper row of **Fig. 2** depicts the combined intensity patterns of the sum of CH_3O^- and $C_2H_5O^-$ fragments from the PHEA of the whole structure on the left and of its smallest spot in the middle. The leftmost image was obtained under static SIMS condition with a probing depth of a few nanometres only. The image of the smallest patterned spot in the middle, was obtained from a dynamic SIMS experiment, eroding the polymer layer down to the silicon wafer. Therefore, the obtained depth-integrated signals of CH_3O^- plus $C_2H_5O^-$ are a measure of the thickness of the deposited polymer spot. The rightmost graph in **Fig. 2** shows the combined intensity of CH_3O^- and $C_2H_5O^-$ across the centre of the smallest structure. The intensity profile has a Gaussian shape with a full width at half of the maximum intensity (FWHM) of around 270 µm and hence no sharp edges. Even though all target structures were rectangles, sharp edges were completely rounded. This smoothing was most pronounced for the smallest structure which was turned into a circle (**Fig. 2**, middle). Increasing the size of the rectangles or grafting of subpatterns

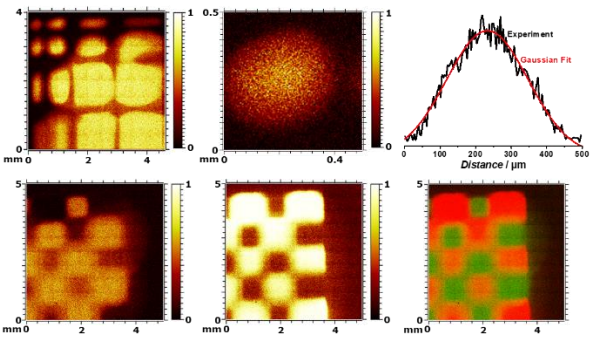

Fig. 2. top: ToF-SIMS data of patterns of PHEA. Intensity patterns of sum of PHEA characteristic CH_3O^- and $C_2H_5O_2^-$ secondary ions of (left) the whole structure and (middle) of its smallest spot. (right): The pseudo profile of the smallest spot from dual beam depth profiling with argon cluster ion erosion. **bottom**: ToF-SIMS spectra of a checkerboard pattern of PtBA and POEGA with the intensity patterns of $C_4H_9O^-$ (left), $C_2H_3O^-$ (middle) and their overlay (right).

in the centre of a bigger pattern led to a loss of lateral resolution, which might be attributed to some low intensity optical artefacts due to undesired reflections. Furthermore, bigger structures showed better-resolved edges and much higher intensities in ToF-SIMS, indicating thicker polymer layers. In contrast to 2-photon direct laser writing, which gains a large portion of its remarkable resolution from the non-linearity of optical susceptibility and light intensity,[32] 1-photon 2D laser lithography completely relies on the beam quality parameter M^2 of the employed laser. The beam quality parameter M^2 gives the deviation factor from a perfectly focusable, thus diffraction limited laser. Our excimer laser featured a rectangular beam with M^2 = 18 and 54, respectively. The minimal theoretical spot size of our set-up ranges around 185 × 96 µm² (refer to the SI for experimental set-up). Given this limitation and the size of the target structure of 236 × 236 µm², a FWHM-diameter of only 270 µm is surprisingly good. Therefore, it is more likely that the resolution of small structures at short exposure times is actually limited by the inhibition by oxygen. Since many commercially available lasers such as diode-pumped Nd:YAG solid-state micro laser have $M^2 < 1.5$, resolutions in the range of 10 µm can be expected for the presented methodology.

In another experiment, a checkerboard pattern of PtBA and POEGA was produced. The bottom row of **Fig. 2** shows the corresponding ToF-SIMS images: the $C_4H_9O^-$ intensity pattern for PtBA (left), the intensity pattern of $C_2H_3O^-$ for POEGMA (middle), and an overlay of both patterns (right). From the latter two it appears that the secondly grafted POEGA formed a better-resolved and more pronounced pattern. In general, the lateral resolution within the checkerboard was much lower than at its borders. This loss of lateral resolution probably led to formation of block copolymers in the centre of the pattern with likely longer inhibition times as similar observations were made for diblock copolymer formation with non-laser UV-light.[24] Inhibition might also be the reason the structures of the first block were more pronounced in the centre of the pattern, whereas the second block was more at its borders. Contrarily to

lateral resolution, film thicknesses close to the edges of the checkerboard pattern seemed much lower than at the centre as evidenced by the presence of a silicon signal in XPS mapping (Fig. S9). Similar to the ToF-SIMS results, XPS mapping evidences a much better resolution for the secondly grafted POEGA at the edges of the checkerboard pattern and concomitantly a much higher presence of PtBA in the centre of the checkerboard.

In conclusion, we introduce the direct grafting of polymer chains in predefined patterns using a focused laser to initiate and control chain growth. Specifically, laser-induced copper-mediated radical polymerization was employed to graft various acrylate monomers from silicon substrates. XPS, ToF-SIMS and GAATR-FTIR evidenced the successful grafting. A linear dependence of the film thickness on direct exposure time to laser light was observed, reaching almost 40 nm after 125 µs of laser light exposure. The controlled nature of the grafting was further demonstrated via block copolymer formation. Moreover, a checkerboard pattern was produced and imaged via ToF-SIMS and XPS. The present methodology is strongly influenced by beam quality of the employed laser and resolutions in the range of 300 µm could be realized according to ToF-SIMS. Better optical set-ups and UV laser with higher beam quality should significantly improve the resolution.

T.J. and J.L. are grateful for funding from the Fonds Wetenschappelijk Onderzoek (FWO) in the form of a project grant and a PhD scholarship. The K-Alpha+ instrument was financially supported by the Federal Ministry of Economics and Technology on the basis of a decision by the German Bundestag. C.B.-K. acknowledges support from the Australian Research Council (ARC) in the form of a Laureate Fellowship, key support from the Queensland University of Technology (QUT) as well as continued support via the STN program of the Helmholtz association at the Karlsruhe Institute of Technology (KIT).

1. Notes and references

1. Z. Nie and E. Kumacheva, *Nat. Mater.*, 2008, **7**, 277-290.
2. S. Hansson, V. Trouillet, T. Tischer, A. S. Goldmann, A. Carlmark, C. Barner-Kowollik and E. Malmstrom, *Biomacromolecules*, 2013, **14**, 64-74.
3. W. H. Binder and R. Sachsenhofer, *Macromol. Rapid Commun.*, 2008, **29**, 952-981.
4. T. Pauloehrl, G. Delaittre, M. Bruns, M. Meissler, H. G. Borner, M. Bastmeyer and C. Barner-Kowollik, *Angew. Chem. Int. Ed.*, 2012, **51**, 9181-9184.
5. T. Pauloehrl, G. Delaittre, V. Winkler, A. Welle, M. Bruns, H. G. Borner, A. M. Greiner, M. Bastmeyer and C. Barner-Kowollik, *Angew. Chem. Int. Ed.*, 2012, **51**, 1071-1074.
6. J. O. Zoppe, N. C. Ataman, P. Mocny, J. Wang, J. Moraes and H. A. Klok, *Chem. Rev.*, 2017, **117**, 1105-1318.
7. R. E. Behling, B. A. Williams, B. L. Staade, L. M. Wolf and E. W. Cochran, *Macromolecules*, 2009, **42**, 1867-1872.
8. O. W. Webster, *Science*, 1991, **251**, 887-893.
9. W. A. Braunecker and K. Matyjaszewski, *Prog. Polym. Sci.*, 2007, **32**, 93-146.
10. M. Zamfir, C. Rodriguez-Emmenegger, S. Bauer, L. Barner, A. Rosenhahn and C. Barner-Kowollik, *J. Mater. Chem. B*, 2013, **1**, 6027-6034.
11. J. Nicolas, Y. Guillaneuf, C. Lefay, D. Bertin, D. Gigmes and B. Charleux, *Prog. Polym. Sci.*, 2013, **38**, 63-235.
12. K. Matyjaszewski, P. J. Miller, N. Shukla, B. Immaraporn, A. Gelman, B. B. Luokala, T. M. Siclovan, G. Kickelbick, T. Vallant, H. Hoffmann and T. Pakula, *Macromolecules*, 1999, **32**, 8716-8724.
13. T. Chen, I. Amin and R. Jordan, *Chem. Soc. Rev.*, 2012, **41**, 3280-3296.
14. C. Wendeln and B. J. Ravoo, *Langmuir*, 2012, **28**, 5527-5538.
15. H. Y. Chen, M. Hirtz, X. Deng, T. Laue, H. Fuchs and J. Lahann, *J. Am. Chem. Soc.*, 2010, **132**, 18023-18025.
16. U. Bog, F. Brinkmann, H. Kalt, C. Koos, T. Mappes, M. Hirtz, H. Fuchs and S. Kober, *Small*, 2014, **10**, 3863-3868.
17. S. Bian, J. He, K. B. Schesing and A. B. Braunschweig, *Small*, 2012, **8**, 2000-2005.
18. N. Kehagias, W. Hu, V. Reboud, N. Lu, B. Dong, L. Chi, H. Fuchs, A. Genua, J. A. Alduncin, J. A. Pomposo, D. Mecerreyes and C. M. S. Torres, *Phys. Status Solidi C*, 2008, **5**, 3571-3575.
19. X. C. Pan, M. A. Tasdelen, J. Laun, T. Junkers, Y. Yagci and K. Matyjaszewski, *Prog. Polym. Sci.*, 2016, **62**, 73-125.
20. J. E. Poelma, B. P. Fors, G. F. Meyers, J. W. Kramer and C. J. Hawker, *Angew. Chem. Int. Ed.*, 2013, **52**, 6844-6848.
21. C. W. Pester, B. Narupai, K. M. Mattson, D. P. Bothman, D. Klinger, K. W. Lee, E. H. Discekici and C. J. Hawker, *Adv. Mater.*, 2016, **28**, 9292-9300.
22. E. H. Discekici, C. W. Pester, N. J. Treat, I. Lawrence, K. M. Mattson, B. Narupai, E. P. Toumayan, Y. D. Luo, A. J. McGrath, P. G. Clark, J. R. de Alaniz and C. J. Hawker, *ACS Macro Lett.*, 2016, **5**, 258-262.
23. G. Ramakers, A. Krivcov, V. Trouillet, A. Welle, H. Mobius and T. Junkers, *Macromol. Rapid Commun.*, 2017, **38**, 1700423.
24. J. Laun, M. Vorobii, A. de los Santos Pereira, O. Pop-Georgievski, V. Trouillet, A. Welle, C. Barner-Kowollik, C. Rodriguez-Emmenegger and T. Junkers, *Macromol. Rapid Commun.*, 2015, **36**, 1681-1686.
25. M. Vorobii, A. de los Santos Pereira, O. Pop-Georgievski, N. Y. Kostina, C. Rodriguez-Emmenegger and V. Percec, *Polym. Chem.*, 2015, **6**, 4210-4220.
26. M. Vorobii, O. Pop-Georgievski, A. D. Pereira, N. Y. Kostina, R. Jezorek, Z. Sedlkova, V. Percec and C. Rodriguez-Emmenegger, *Polym. Chem.*, 2016, **7**, 6934-6945.
27. P. Mueller, M. M. Zieger, B. Richter, A. S. Quick, J. Fischer, J. B. Mueller, L. Zhou, G. U. Nienhaus, M. Bastmeyer, C. Barner-Kowollik and M. Wegener, *ACS Nano*, 2017, **11**, 6396-6403.
28. S. Telitel, S. Telitel, J. Bosson, A. Spangenberg, J. Lalevee, F. Morlet-Savary, J. L. Clement, Y. Guillaneuf, D. Gigmes and O. Soppera, *Adv. Mater. Interfaces*, 2014, **1**, 1400067.
29. S. Telitel, F. Dumur, S. Telitel, O. Soppera, M. Lepeltier, Y. Guillaneuf, J. Poly, F. Morlet-Savary, P. Fioux, J. P. Fouassier, D. Gigmes and J. Lalevee, *Polym. Chem.*, 2015, **6**, 613-624.
30. R. Barbey, L. Lavanant, D. Paripovic, N. Schuwer, C. Sugnaux, S. Tugulu and H. A. Klok, *Chem. Rev.*, 2009, **109**, 5437-5527.
31. S. Turgman-Cohen and J. Genzer, *J Am Chem Soc*, 2011, **133**, 17567-17569.
32. C. Barner-Kowollik, M. Bastemeyer, E. Blasco, M. Patrick, G. Delaittre, B. Richter and M. Wegener, *Angew. Chem. Int. Ed.*, 2017, DOI: 10.1002/anie.201704695.

